Optics Communications 439 (2019) 112–117

Contents lists available at ScienceDirect

Optics Communications

journal homepage: www.elsevier.com/locate/optcom

Why elliptic microcavity lasers emit light on bow-tie-like modes instead of whispering-gallery-like modes☆

Alexander O. Spiridonov [a], Evgenii M. Karchevskii [b], Trevor M. Benson [c], Alexander I. Nosich [d,*]

[a] Laboratory of Computational Technologies and Computer Modeling, Kazan Federal University, Kazan, 420008, Russia
[b] Department of Applied Mathematics, Kazan Federal University, Kazan, 420008, Russia
[c] George Green Institute for Electromagnetics Research, The University of Nottingham, Nottingham NG9 7RD, UK
[d] Laboratory of Micro and Nano Optics, Institute of Radio-Physics and Electronics NASU, Kharkiv 61085, Ukraine

ARTICLE INFO

Keywords:
Microcavity laser
Threshold gain
Muller boundary integral equation
Bow-tie-like mode
Whispering-gallery-like mode

ABSTRACT

We study numerically a two-dimensional (2-D) elliptical microcavity laser, in the center of which a circular active region is located, modeling a focused pumped spot or an injection electrode. The object of the research is to study lasing spectra, gain-medium thresholds, and modal fields, found as solutions to a classical electromagnetic eigenvalue problem tailored to address the threshold conditions. The instrument of our study is the set of two coupled Muller boundary integral equations (BIE) on the boundaries of the cavity and the active region. These BIEs are discretized by the Nystrom technique that guarantees the convergence. Among the modes that co-exist in such a resonator, we demonstrate the whispering-gallery-like modes (WGM) and the bow-tie-like modes (BTM). We find that the threshold values of material gain of BTMs can become lower than those of nearby WGMs if the radius of the active region in the cavity center is getting sufficiently small.

1. Introduction

Microcavity lasers have been the object of active research since the 1990s. 2-D microlasers appear as reasonable approximations to 3-D configurations shaped as thin flat "disks" or "patches" thanks to the effective refractive index concept. Their natural modes were analyzed as complex-frequency eigenvalue problems for Maxwell's equations using a variety of techniques — see reviews [1–5]. Although useful, passive-cavity models neglect gain and hence cannot characterize the threshold of lasing.

An important example of the shortcoming of these passive models is in the description of a phenomenon discovered in the late 1990s when so-called stadium lasers were proposed [6], providing better directionality than circular-disk ones. Later dye-doped polymer lasers of this shape were also fabricated and measured [7,8]. In contrast to the common belief that the lasing always occurs on the highest-Q modes, it was found that these lasers emitted light on bow-tie-like (BTM-like) modes instead of whispering-gallery-like modes (WGM-like) ones (perturbed WGMs) despite the much higher Q-factors of the latter. Although some of these papers did not mention BTMs explicitly, their presence was always betrayed by the presence of four similar beams in the far-field angular emission patterns. This mystery was widely admitted however has not yet apparently obtained satisfactory explanation although, to address it, nonlinear theories involving rate equations were developed. One of the factors preventing such an explanation can be seen as the absence of an adequate classical electromagnetic model.

In large passive 2-D dielectric cavities, BTMs were studied both via an approximate billiard-theory approach [1,3,4,6,7] and using more accurate techniques based on the boundary IEs [9]. Although some of these IEs contained spurious (purely real) eigenvalues, and were solved by brute-force numerical algorithms (for details, see [10]), this yielded important result: BTM-like modes were found in flattened quadrupole, stadium, and elliptic dielectric micro-cavities. Being quite different from the viewpoint of the ray-tracing billiard theory, within the full-wave optics all these shapes can be viewed as smooth perturbations of a circle by means of the elongation along one of the two symmetry axes. Then, the theory of the Fredholm operator-valued functions leads to conclusion that both WGM-like and BTM-like modes exist in either of these shapes if their difference is small, in certain norm. In particular, the nature of BTMs was connected to the coupling of the formerly decoupled modes of the circle with different azimuthal indices that appeared due to such elongation.

These studies, however, were unable to answer the question of why the lasing was observed on BTMs instead of WGMs. A remarkable citation from [3], p. 254 is, "Lasing of bow-tie modes has also posed a theoretical question: why do the bow-tie modes always lase although there exist many other 2D patterns of resonance modes than bow-tie

☆ This research did not receive any specific grant from funding agencies in the public, commercial, or not-for-profit sectors.
* Corresponding author.
E-mail address: anosich@yahoo.com (A.I. Nosich).

https://doi.org/10.1016/j.optcom.2019.01.056
Received 30 October 2018; Received in revised form 31 December 2018; Accepted 19 January 2019
Available online 24 January 2019

modes?" Our work presented below is aimed at the explanation of that phenomenon from the viewpoint of mode thresholds.

In our analysis of the threshold conditions, we use a specific electromagnetic model adapted to study the lasing of the open resonators equipped with active regions. It is called the Lasing Eigenvalue Problem (LEP), the detailed statement of which can be found in [10,11]. This is the eigenvalue (i.e. source-free) electromagnetic field boundary value problem specifically tailored to provide both the modal wavelengths and the associated values of threshold material gain in the active region. This is because, in contrast to the conventional eigenvalue problem considering the complex modal frequencies (and associated Q-factors) for a passive optical cavity, the LEP fully takes into account the size, shape and location of the active region. As shown in [11], every LEP eigenvalue automatically satisfies both the "gain = loss" and the "phase conjugation" conditions, which appear as the real and the imaginary parts, respectively, of the Poynting theorem applied to the laser mode field. Therefore the LEP formalism is, in fact, the full-wave classical (i.e. purely electromagnetic) laser threshold theory equally valid for any 2-D and 3-D configuration. Here it should be noted that the so-called "semi-classical theory", developed at the onset of laser studies when early laser resonators were measured in thousands of wavelengths, coincides with the LEP for the 1-D laser models, which involve only flat-layered infinite-width micro-cavities (see [11]).

To date the LEP approach has been successfully applied to a variety of 2-D stand-alone micro-lasers in the form of an active circle [11], ellipse [12], limacon [13], and kite [10], active cyclic photonic molecules [14], active circular disks with passive annular Bragg reflectors [15], and a partially active circle [16]. More recently the LEP was applied to the modes of a single plasmonic nanostrip [17] and a plasmonic nanotube [18] placed into an active circular shell, which can be viewed as a quantum wire. An infinite array of circular quantum nanowires was considered with the LEP in [19], where it was shown that such a periodic open active resonator can support so-called lattice modes with ultra-low thresholds and wavelengths located near to the Rayleigh anomalies. A similar LEP-based study of the lasing modes of an infinite binary grating of circular silver and quantum nanowires was published in [20] where the thresholds of the localized surface plasmon (LSP) modes were found to be higher than those of the lattice modes.

Note also that there exist other LEP-like formulations aimed at the extraction of mode threshold, see [21–23]; some of them differ from the LEP only by the choice of the material-gain parameter, which can be regarded as the imaginary part of the dielectric permittivity rather than the imaginary part of the refractive index, or as the product of the wavenumber and the imaginary part of the refractive index. In any case the principal step is the assumption that the threshold value of gain is unknown and considered as eigenvalue. This is fully adequate to the fundamental observation, known from the onset of laser research, that the thresholds of lasing are closely tied to the field patterns of open cavity modes and their overlap with the active region.

Note that the LEP formalism is especially advantageous in the analysis of micro-cavity lasers where active regions do not coincide with the whole cavity, for instance due to the application of a well-focused optical pump or a shaped carrier-injection electrode.

2. Problem formulation and outline of solution

The object of our study is the electromagnetic field depending on time as $\exp(-i\omega t)$, where ω is the angular frequency, in the presence of an open dielectric resonator, shown in Fig. 1 and made of non-magnetic materials. We assume that the active region is the inner domain Ω_1, which contains a gain material with a complex-valued refractive index $\nu = \alpha - i\gamma$, where $\alpha > 0$ is known and $\gamma > 0$ is unknown. The outer domain Ω_2 has the same refractive index $\alpha > 0$ (known value) and the host medium refractive index is 1 (domain Ω_e). Denote the free-space wavenumber as $k = \omega/c$, where c is the light velocity. A function U is called the eigenfunction of the LEP generated by the real-valued

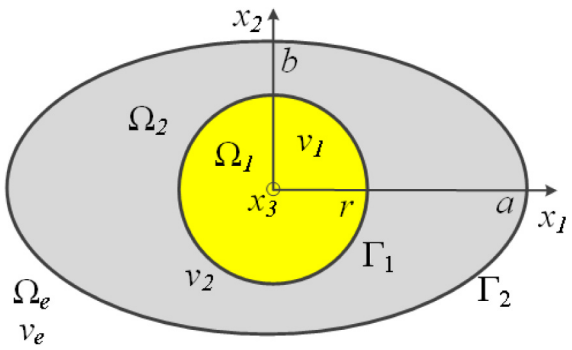

Fig. 1. Geometry of a 2-D elliptic dielectric resonator with a circular active region inside.

eigenpair (k, γ) provided that it satisfies the Helmholtz equation in $\Omega_{1,2}$ and host medium with corresponding wavenumbers, the tangential electromagnetic-field components continuity conditions at the contours of the active region Γ_1 and the cavity Γ_2, and, thanks to the real k, the Sommerfeld radiation condition far from the cavity.

As it was noted in [11], the theory of analytic operator-valued functions allows one to find that, for arbitrary micro-cavity with arbitrary active region, the set of the eigenvalue pairs (k_s, γ_s) is discrete ($s = 1,2,\ldots$), the multiplicity of each eigenvalue is finite, they cannot appear or disappear in the domain of problem's analyticity, and the only point of their accumulation is at infinity. In order to find them numerically, a trusted computational tool should be used. As such a tool, we use the Muller BIE, which (i) is fully equivalent to the original boundary-value problem, (ii) has no spurious eigenvalues, and (iii) is of the Fredholm second kind, i.e. it has smooth and square-integrable kernels.

Keeping this in mind and following [10], we reduce the LEP to the eigenvalue problem corresponding to the following operator equation:

$$(\mathbf{I} + \mathbf{B}(k, \gamma))\,\mathbf{W} = 0, \tag{1}$$

where $\mathbf{W}$ is the vector of four functions corresponding to the field components tangential to two curves $\Gamma_{1,2}$, $\mathbf{I}$ is the identity operator, and $\mathbf{B}$ is an operator-valued function of k, γ involving weakly singular integral operators (if $\Gamma_{1,2}$ are at least twice continuously differentiable). Explicit expressions for all involved quantities can be found in [24]. Then (1) is a generalized spectral problem (in a mathematical sense) for the Fredholm operator-valued function.

To find the spectrum of eigenvalues, we discretize (1) numerically using the Nystrom method in the form first proposed in [10]; we use the improved version that takes account of possible symmetries of the contours [12,24]. Then the search for the LEP eigenvalues is reduced to the calculation of the zeros of the determinant generated by the matrix equation obtained from (1). Further, we take into account that, according to the matrix algebra (see [25], Theorem 7.3.5), these zeros coincide with the zeros of the inverse condition number of the same matrix. As computing the condition number of an arbitrary matrix is more favorable than finding its determinant, we analyze the former quantity as a function of parameters.

The search for eigenvalues is done by the iterative method. To verify the code, we used the lasing frequencies and thresholds of the modes of uniformly active circular and elliptic micro-cavities from [11] and [12] as reference data. Note that, unlike some other forms of BIE, the Muller BIE has no false eigenvalues and the exponential convergence of the Nystrom method when taking larger orders of discretization is guaranteed mathematically [10]. Hence the accessible accuracy, controlled by that order, is limited only by the machine precision. Initial results of our work were presented in the conference paper [24]; here we support them with larger numerical data and make better grounded conclusions.

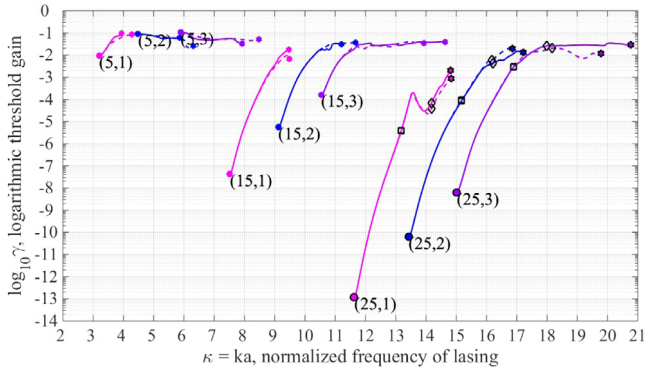

Fig. 2. Dependences of the lasing frequencies and threshold gains of the H-polarized modes of the fully active elliptic cavity on the axes ratio b/a varying between 1 (circle) and 0.5. Solutions for $b/a = 1$, 0.75, 0.6, and 0.5, are marked with circles, squares, rhombuses, and stars, respectively. The solid lines correspond to the eigenvalues of the x-even modes while the dashed lines to the eigenvalues of the x-odd modes.

3. Numerical results and discussion

For systematic computations, we have chosen the elliptic cavity with the axes ratio $b/a = 0.5282$ and a circular active region of the relative radius r/a taking values from 0.1585 to 0.4577 and located in the ellipse center. In computations, we take the cavity refractive index as $\alpha = 2.63$ that corresponds, for instance, to the effective refractive index of GaAs layer of thickness 200 nm at the optical-communication wavelength of 1550 nm.

It should be noted that, in an elliptic cavity, there is no obvious way of assigning the mode indices as exists for a circular cavity. As is known, the two-index notation (m, n) is commonly used for a circle: the first index is the azimuthal index, and the second is the radial index; in a circle, they correspond to the numbers of the mode field variations. Therefore, we consider an elliptic cavity as a smooth deformation of the circle and preserve these indices even in the deformed cavity case where they lose such a simple physical meaning.

It is necessary to stress that in a fully active (flood-pumped) elliptic cavity BTMs do not dominate over WGMs, in the sense of the threshold gain values. This is demonstrated by the curves in Fig. 2 that are the trajectories, on the plane (ka, γ), of the LEP eigenvalues for the modes of active circle $(a/b = 1)$ continuously transforming to the modes of active ellipse with the axes ratio $b/a = 0.5$.

The calculations demonstrate that both the x-even and the x-odd WGM-like modes of the fully active elliptic cavity with indices (25,1) keep having the field patterns typical of the WGMs, although distorted by the deformation from circle to ellipse, and remarkably low thresholds. In contrast, for b/a less or equal to 0.6 the x-even (25, 2) and the x-odd (25, 3) modes obtain, in elliptic cavity, the field patterns corresponding to BTMs and nearly two orders higher thresholds (see Fig. 2).

Turning now to the cavity with partial active region shaped as a circle in the cavity center, we find that if active region the shrinks in size, there is little effect on all the mode frequencies (Fig. 3(a)).

The mode thresholds are affected much more strongly: they grow up and WGM thresholds quickly obtain dramatically high values while the BTM thresholds change moderately (Fig. 3(b)). As a result, for any pair of such modes one can find a small enough radius of the active region in the cavity center that provides a lower threshold of a BTM than that of a WGM. The explanation of this behavior is quite clear after [11] (see eq. (37)): the mode threshold gain is inversely proportional to the product of passive-cavity Q-factor and the overlap coefficient $\Gamma_s^{(gain)} \leq 1$ between the passive-cavity mode E-field and the active region,

$$\gamma_s = \frac{\alpha}{\Gamma_s^{(gain)} Q_s} + O(\gamma_s^2), \quad \text{if } \gamma_s << 1. \tag{2}$$

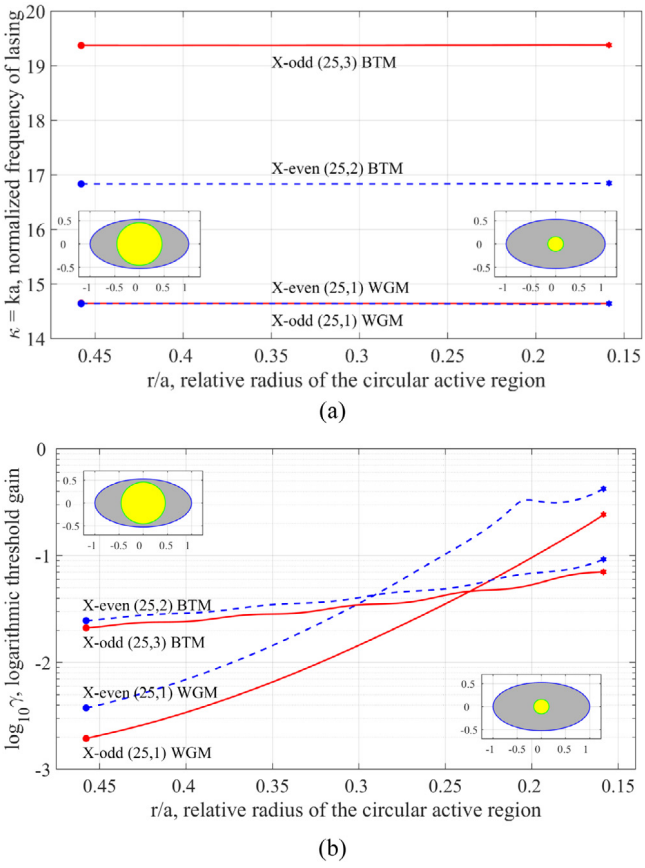

Fig. 3. Dependences of the lasing frequencies (a) and the threshold gains (b) of the H-polarized BTMs and WGMs of elliptic resonator with circular active region on the relative radius of the latter, r/a.

It is the overlap coefficient that is strongly corrupted for WGMs if the pump is applied in a small circle in the ellipse center; however remains almost intact for BTMs. This leads to the sharp rise in the thresholds of WGMs and apparently makes the BTMs the first modes to exhibit lasing in the experiments.

In Fig. 4, we show the near- and far-field patterns of the H-polarized X-even and X-odd WGMs (25,1), for $b/a = 0.5282$ and two different active circle radii: $r/a = 0.4577$ (large) and 0.1585 (small). The features of WGMs are clearly observable for both large and small circular active regions.

Systematic computations have shown that BTM solutions of the LEP can be found only in the elliptic dielectric cavities with the axes ratio around or smaller than $b/a = 0.6$. Keeping in mind that the elliptic cavity is considered as a smooth deformation of circle, we have found that the BTM solutions are always obtained as deformations of the modes of a circular cavity with radial indices $n > 1$. In contrast, the WGM solutions are always obtained from the modes of a circle having $n = 1$.

In Fig. 5, we show the near-field patterns of the H-polarized X-even (25, 2) BTM and X-odd (25, 3) BTM, for the same two values of the normalized radius of the active region as in Fig. 4. The characteristic field patterns of the BTMs are equally well observable for the active regions of any radius, both large and small. As mentioned above, in the latter case BTMs can have moderate and even smaller values of threshold gain than the WGM solutions. In the far zone, BTMs display a specific "signature" in the form of emission patterns with four symmetric intensive beams (see [1,6,7]). Still these beams are not clearly the dominant ones because the computed cavities have moderate size (15 wavelengths in material) in comparison to experimentally measured ones (over 100 wavelengths).

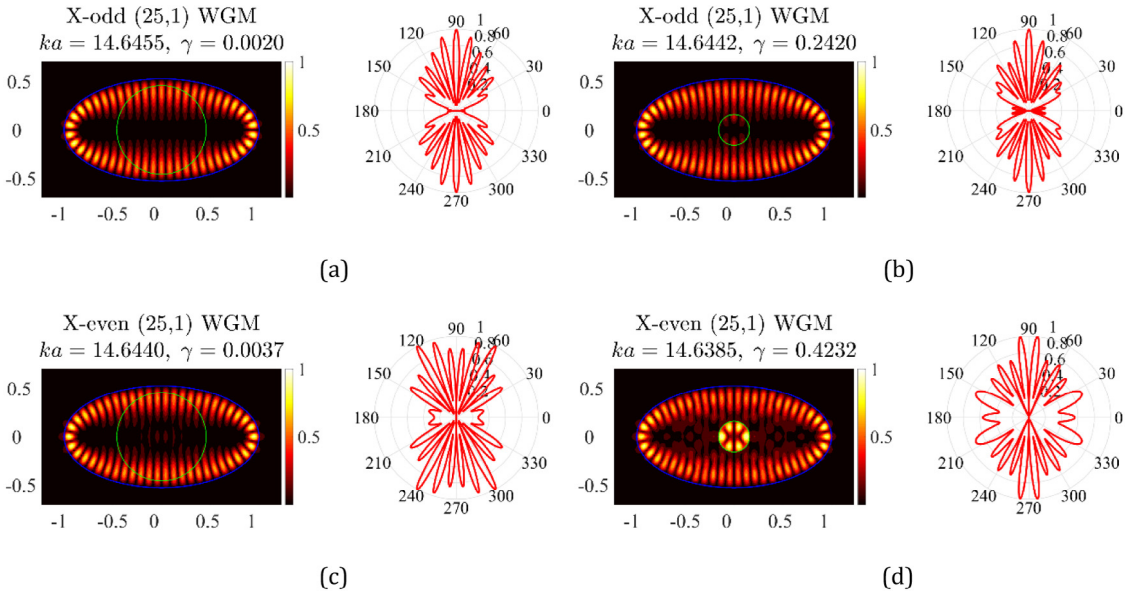

Fig. 4. Near fields and far-field emission patterns of WGMs of the X-odd (upper pair) and X-even (lower pair) symmetry classes of the elliptical cavity with a circular active region of large and small radius (shown by green circle). WGM features are clearly observable. (For interpretation of the references to color in this figure legend, the reader is referred to the web version of this article.)

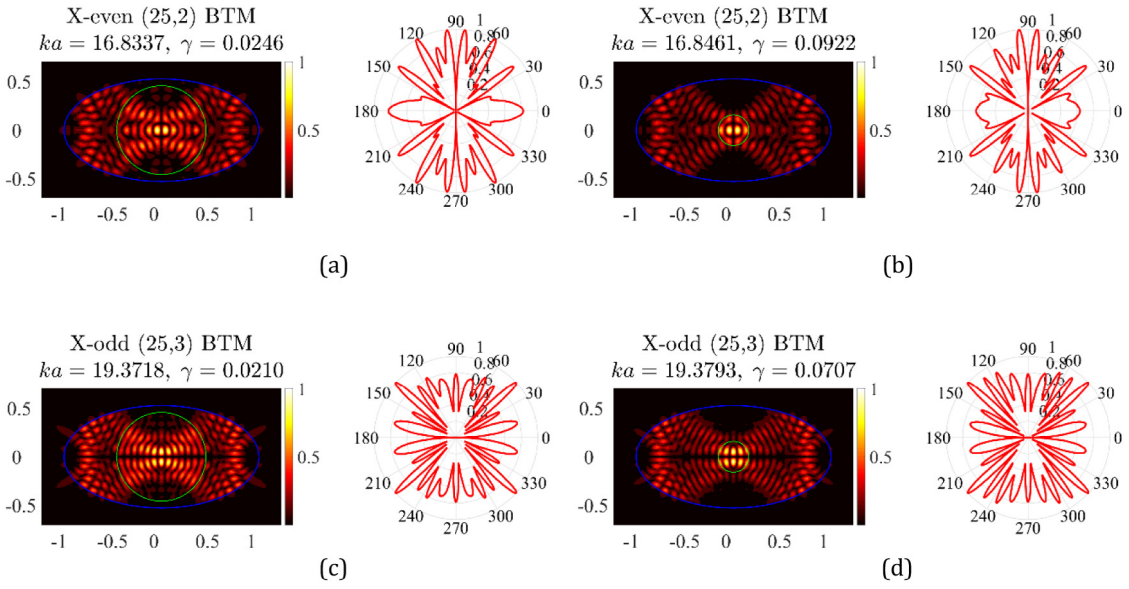

Fig. 5. The same as in Fig. 4 however for BTMs of the X-even (upper pair) and X-odd (lower pair) symmetry classes of the elliptical resonator with a circular active region.

Another common feature is that the deformation from circle to ellipse leads to the well observable growth of the magnitude of the field hot spots at the parts of contour where its curvature is the largest, i.e. near to the apexes of the main axis. The field pattern is quite stable with respect to variations in the active-region radius. Still the smaller the radius of the active circle, the higher the thresholds; this means the appearance of a noticeable gain-induced contrast between active and passive regions of ellipse. Indeed, the lower panel of Fig. 4 shows that, in the case of the X-odd mode (25,1), the presence of small-radius active region leads to appearance of an additional WGM-like pattern in the active region itself; such a pattern resembles the mode (3,1) of a circular cavity.

Such hybridization of modes of partial domains with different refractive indices is known in other types of micro-cavities [11,15,18]. Thanks to this effect, the modes of composite cavities are also called "supermodes". Still it is interesting to see that in our case the hybridization can take place even if the optical contrast is created only by the presence of the gain in the pumped region.

To give a broader view of the comparative analysis of WGM and BTM thresholds of lasing in elliptic micro-cavities with partial active regions, we present two-color maps of the mentioned above quantity, $1/\mathrm{cond}[\mathbf{I} + \mathbf{B}(ka, \gamma)]$, as a function of two variables, ka and γ. They correspond to a large (Fig. 6) and a small (Fig. 7) radius of the active circle in the center of the ellipse. This comparison reveals an amazing result: in each case, one can see that there exists an almost periodic in frequency sequence of modes, which have much lower thresholds than all others. They are WGM-like modes in Fig. 6, for a large active region, and BTM-like modes in Fig. 7 for a small active region.

The analysis presented above explains, as we believe, the mystery around the performance of the stadium and similar-shape 2-D lasers:

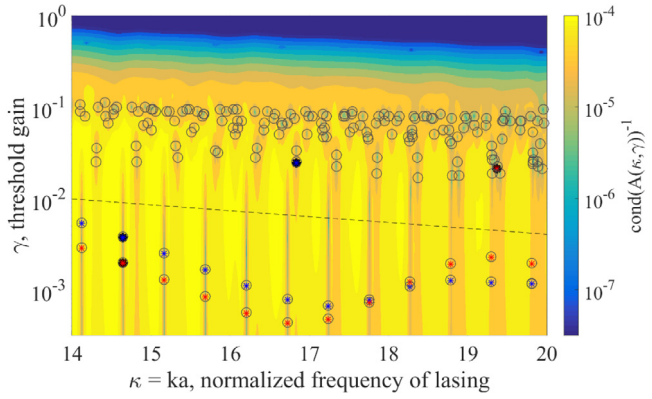

Fig. 6. Semi-log color map of the inverse condition number on the plane (ka, γ) for an elliptic resonator with a wide circular active region of $r/a = 0.4577$, H-polarization case. The circles mark the local minima on the map. The red stars correspond to the X-odd modes and the blue stars to the X-even modes. Note that all the lowest-threshold modes located below the dotted line are WGMs. (For interpretation of the references to color in this figure legend, the reader is referred to the web version of this article.)

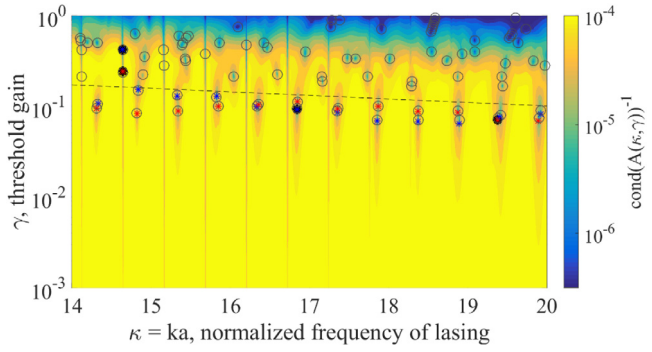

Fig. 7. The same as in Fig. 6 but for an elliptic resonator with a narrow circular active region of $r/a = 0.1585$, Note that all the lowest-threshold modes located below the dotted line are BTMs.

despite much higher Q-factors (in a passive cavity) of WGMs, the lasing (in the active cavity, i.e. under pumping) occurs on the BTMs. As we have already mentioned, this happens apparently because the modal overlap with a small active region in the cavity center is much better with BTMs than with WGMs. Indeed, the micro image of the stadium laser in Fig. 1 of [6] shows the injection electrode in its center, following the cavity shape with the ratio 1:2. Such an electrode did not overlap with the field of any high-Q perturbed WGM however overlapped well with BTM fields, similar to our analysis.

This explanation could be questioned for the polymer stadium lasers of [7] where the pumping was done optically and in a flood manner, so that illumination of the cavity was uniform. However, according to [26], the reactive ion etching used for shaping the dye-doped polymer samples resulted in a clearly observable bleaching of the cavity rim. That bleaching, in fact, re-shaped the active region and one can guess post factum that such re-shaping was sufficient to spoil the lasing of WGMs. This is because, in a 100-lambda stadium cavity laser measured in [7], the fields of high-Q WGMs (with $m >> 1$) were tightly compressed at the rim. In contrast, the explained bleaching of the rim did not affect the BTMs, which overlapped well even with reduced active region.

4. Conclusions

Summarizing, we have for the first time quantified numerically, using the LEP formulation, the emission frequencies and threshold values of material gain for the 2-D elliptic micro-cavity laser with a circular active region. We have used the coupled weakly-singular Muller BIEs discretized with the aid of the Nystrom technique that guarantees the convergence of computations. Our analysis has shown that the most common modes in elliptic cavities with sufficiently large eccentricity (and apparently in other similarly elongated cavities such as stadium and quadrupole geometries) are the WGM-like and the BTM-like ones, with their corresponding characteristic near-field patterns. For a uniformly active cavity, WGMs have considerably lower thresholds than BTMs. However this is not true anymore if the active region in such a micro-laser (i.e. photo-pumped spot or injection electrode) does not coincide with the whole cavity but is a circle located at the cavity center. In such a case, a reduction of the active-region radius raises the threshold values of gain for WGMs in a dramatic manner, unlike those for BTMs which thus can become the lowest threshold ones. This apparently explains the experimental behavior of the stadium-like micro-cavity lasers and shows that an active region's shape, size and location offer an efficient tool with which to engineer the lasing thresholds of various micro-cavity lasers.

References

[1] K.J. Vahala, Optical microcavities, Nature 424 (2003) 839–846.
[2] A.I. Nosich, E.I. Smotrova, S.V. Boriskina, T.M. Benson, P. Sewell, Trends in microdisk laser research and linear optical modelling, Opt. Quantum Electron. 39 (2007) 1253–1272.
[3] T. Harayama, S. Shinohara, Two-dimensional microcavity lasers, Laser Photonics Rev. 5 (2011) 247–281.
[4] L. He, S.K. Ozdemir, L. Yang, Whispering gallery microcavity lasers, Laser Photonics Rev. 7 (2013) 60–82.
[5] Y.-D. Yang, Y.-Z. Huang, Mode characteristics and directional emission for square microcavity lasers, J. Phys. D: Appl. Phys. 49 (2016) 253001.
[6] C. Gmachl, F. Capasso, E.E. Narimanov, J.U. Nockel, A.D. Stone, J. Faist, D.L. Sivco, A.Y. Cho, High-power directional emission from microlasers with chaotic resonators, Science 280 (1998) 1556–1664.
[7] M. Lebental, J. Lauret, J. S. Zyss, C. Schmit, E. Bogomolny, Directional emission of stadium-shaped microlasers, Phys. Rev. A 75 (2007) 033806.
[8] W. Fanga, H. Cao, Wave interference effect on polymer microstadium laser, Appl. Phys. Lett. 91 (2007) 041108.
[9] R. Dubertrand, E. Bogomolny, N. Djellali, M. Lebental, C. Schmit, Circular dielectric cavity and its deformations, Phys. Rev. A 77 (2008) 013804.
[10] E.I. Smotrova, V. Tsvirkun, I. Gozhyk, C. Lafargue, C. Ulysse, M. Lebental, A.I. Nosich, Spectra, thresholds, and modal fields of a kite-shaped microcavity laser, J. Opt. Soc. Amer. B 30 (2013) 1732–1742.
[11] E.I. Smotrova, V.O. Byelobrov, T.M. Benson, J. Ctyroky, R. Sauleau, A.I. Nosich, Optical theorem helps understand thresholds of lasing in microcavities with active regions, IEEE J. Quantum Electron. 47 (2011) 20–30.
[12] A.O. Spiridonov, E.M. Karchevskii, A.I. Nosich, Symmetry accounting in the integral-equation analysis of the lasing eigenvalue problems for two-dimensional optical microcavities, J. Opt. Soc. Amer. B 34 (2017) 1435–1443.
[13] E.I. Smotrova, A.I. Nosich, Thresholds of lasing and modal patterns of a limacon cavity analysed with Muller's integral equations, in: Proc. Int. Conf. Laser and Fiber-Optics Numerical Modeling, LFNM-11, Kharkiv, 2011, art. no. 083.
[14] E.I. Smotrova, A.I. Nosich, T.M. Benson, P. Sewell, Threshold reduction in a cyclic photonic molecule laser composed of identical microdisks with whispering-gallery modes, Opt. Lett. 31 (2006) 921–923.
[15] E.I. Smotrova, T. Benson, P. Sewell, J. Ctyroky, A.I. Nosich, Lasing frequencies and thresholds of the dipole-type supermodes in an active microdisk concentrically coupled with a passive microring, J. Opt. Soc. Amer. A 25 (2008) 2884–2892.
[16] A.S. Zolotukhina, A.O. Spiridonov, E.M. Karchevskii, A.I. Nosich, Electromagnetic analysis of optimal pumping of a microdisk laser with a ring electrode, Appl. Phys. B 123 (32) (2017).
[17] O.V. Shapoval, K. Kobayashi, A.I. Nosich, Electromagnetic engineering of a single-mode nanolaser on a metal plasmonic strip placed into a circular quantum wire, IEEE J. Sel. Top. Quantum Electron. 23 (2017) 1501609.
[18] D.M. Natarov, T.M. Benson, A.I. Nosich, Electromagnetic analysis of the lasing thresholds of hybrid plasmon modes of a silver tube nanolaser with active core and active shell, Beilstein J. Nanotechnol. 10 (2019).
[19] V.O. Byelobrov, J. Ctyroky, T.M. Benson, R. Sauleau, A. Altintas, A.I. Nosich, Low-threshold lasing modes of infinite periodic chain of quantum wires, Opt. Lett. 35 (2010) 3634–3636.
[20] V.O. Byelobrov, T.M. Benson, A.I. Nosich, Binary grating of sub-wavelength silver and quantum wires as a photonic-plasmonic lasing platform with nanoscale elements, IEEE J. Sel. Top. Quantum Electron. 18 (2012) 1839–1846.
[21] A. Mock, First principles derivation of microcavity semiconductor laser threshold condition and its application to fdtd active cavity modeling, J. Opt. Soc. Amer. B 27 (2010) 2262–2272.
[22] S.W. Chang, Confinement factors and modal volumes of micro and nanocavities invariant to integration regions, IEEE J. Sel. Top. Quantum Electron. 18 (2012) 1771–1780.
[23] D. Gagnon, J. Dumont, J.-L. Deziel, L.J. Dube, Ab initio investigation of lasing thresholds in photonic molecules, J. Opt. Soc. Amer. B 31 (2014) 1867–1873.

[24] A.O. Spiridonov, E.M. Karchevskii, Field patterns of whispering-gallery and bow-tie modes of elliptic microcavity laser with a circular active region, in: Proc. Int. Conf. Transp. Opt. Networks, ICTON-2016, Trento, 2016, p. 7550639.

[25] R.A. Horn, C.R. Johnson, Matrix Analysis, Cambridge Univ. Press, Cambridge, 2013.

[26] M. Lebental, Université Paris-Saclay, France, Private communication.